JOURNAL OF CATALYSIS 148, 524–533 (1994)

Characterization of H–Y and Cr–Y Zeolite Catalysts during the Oxidative Destruction of CFC11 and CFC12

Swati Karmakar and Howard L. Greene[1]

Department of Chemical Engineering, The University of Akron, Akron, Ohio 44325-3906

Received October 4, 1993; revised February 28, 1994

The long term stability–deactivation characteristics of two Y zeolite catalysts, namely H–Y and cation exchanged Cr–Y, were studied during the oxidative destruction of CFC11 and CFC12 feeds. Experiments were carried out at 300°C and 5000 h^{-1} space velocity. Properties of the catalysts including activity, selectivity, surface area, acidity, composition, and crystallinity were determined as a function of reaction time. Comparison of these properties with time indicated a significantly higher degree of deactivation for the H–Y catalyst than for the Cr–Y catalyst. The most probable reasons for the improved stability characteristics of the Cr–Y catalyst were the greater stability of the zeolite matrix due to multivalency of the exchanged Cr cation, and also the Deacon reaction characteristic of Cr^{3+}, which converted HCl produced during the destruction of CFCs into Cl_2, thereby restoring the zeolite acid sites.

INTRODUCTION

In our earlier investigations (1–3), it was found that Y zeolite catalysts, especially in the cation exchanged forms such as Co–Y, Cr–Y, etc., were very active for the oxidative destruction of hazardous chlorinated hydrocarbons such as carbon tetrachloride, methylene chloride, and trichloroethylene. The primary reaction products in the presence of water as a cofeed were HCl, CO, CO_2, and traces of Cl_2. The successful use of Y zeolite catalysts for this application subsequently led to investigation of the applicability of these catalysts for the oxidative destruction of chlorofluorocarbons (CFCs).

Preliminary results (4) showed that although the initial activities of the Y zeolite catalysts tested were excellent for the oxidative destruction of CFC11 (CCl_3F) and CFC12 (CCl_2F_2) feeds, catalyst stability was a problem of major concern. Corrosive reaction products such as HF, F_2, and Cl_2 were thought to be primarily responsible for much of the catalyst deactivation. For the experiments involving CFC feeds, no water was added in the reactant stream in an attempt to avoid the formation of HF, as it reacts more readily with silica (one of the major constituents of Y zeolite) than does dry F_2. However, detection of HCl in the effluent indicated participation of zeolite hydroxyls in the oxidation reaction of CFCs. Any F_2 and HF formed were largely retained by the catalyst and were not detected in the effluent.

It was also observed (4) that cation exchange of the H–Y zeolite with chromium to produce Cr–Y substantially improved the catalyst stability against halogen deactivation. Kowalak *et al.* have also reported (5–8) improved stability of polyvalent cation exchanged zeolites (namely Al–Y), as compared to H–Y, during fluorine modification of zeolite Y catalysts. Polyvalent cations in zeolite Y are bonded to more than one alumina tetrahedron and are suggested to provide greater structural stability. It is also possible that the Deacon reaction [$4HCl + O_2 = 2Cl_2 + 2H_2O$], catalyzed by the Cr^{3+} ions present in the Cr–Y zeolite, was responsible for conversion of halogen acids (produced during the oxidative destruction of CFCs) to free halogens (as no Cl_2 was detected from H–Y, but only from Cr–Y). This mechanism would restore the zeolite hydroxyls, thereby conferring better stability characteristics on the Cr–Y zeolite.

It was subsequently decided to compare and document the changes in the catalytic and physical properties of the H–Y and the Cr–Y zeolite catalysts that occurred during the dry oxidative destruction of CFC11 and CFC12 feeds. Additional studies to investigate the effect of adding water vapor to the reactant stream on the stability of the zeolite catalyst are in progress now and will be reported later.

Fevrier *et al.* (9) studied the sorption of certain CFCs, namely CFC11, CFC12, CFC22, CFC113, etc., on 13× molecular sieves, a crystalline aluminosilicate similar to zeolite Y. The results showed simultaneous sorption of and reaction between CFCs and the molecular sieve producing CO_2 and halogen acids.

Although no other literature was directly available on the effects which reacting CFCs might have on the various properties of zeolite catalysts, some related information was found. For example, fluorine in many forms has

[1] To whom correspondence should be addressed.

0021-9517/94 $6.00

been used as a catalyst promoter for zeolites as well as for other metal oxide catalysts (5–8, 10–24). Vapor phase fluorination and impregnation are the two common methods of incorporating fluorine into the catalysts. In vapor phase fluorination, fluorine-containing gases such as F_2, HF, NH_4F, CF_4, CHF_3, $CClF_3$, etc. are diluted with an inert gas such as N_2 or He and are sent through a reactor containing the catalyst at a temperature between ambient and 500°C. Impregnation by soaking the catalyst with an aqueous solution of HF or NH_4F followed by calcination at a higher temperature is also used to enhance activity of zeolite and metal oxide based catalysts. In most of these cases, mild fluorination has been found to improve catalyst acidity and hence activity for acid catalyzed reactions. Partial replacement of surface oxygen or hydroxyl groups by extremely electronegative fluorine increases the polarity of the lattice and hence the strength of the remaining surface hydroxyl sites. Prolonged fluorination, however, has been reported (11, 18) to cause considerable deterioration in activity of both the zeolite and the metal oxide catalysts by replacing most of the lattice oxygens with fluorine.

The present study is an attempt to understand the process of catalyst deactivation by studying changes in catalyst properties caused by the attack of reactive halogens and halogen acids produced during the oxidative destruction of CFC11 and CFC12. These changes have been documented using acidity determination by NH_3 TPD, surface area measurement by BET, and structural analysis by IR spectroscopy and XRD.

EXPERIMENTAL

H–Y zeolite pellets ($\frac{1}{16}$-in. extrudates) were used as received from UOP. for the experiments involving the H–Y catalyst. Cr–Y catalyst pellets were prepared from the H–Y pellets by standard cation exchange procedures (4, 25). The Cr–Y pellets, prepared by cation exchanging the H–Y pellets, were calcined at 500°C overnight before they were subjected to any experiments.

The deactivation studies were carried out in a vertical Pyrex tubular reactor (31 mm o.d., 27 mm i.d., and 1 m length), a schematic of which has been shown elsewhere (4). The reactor had a preheater section for preheating the feed gases and a fixed bed catalyst section where the reactions took place. For all the experiments, a feed concentration of 1500–2000 ppm of CFC in air was utilized. To feed CFC12 (b.p. −29.8°C) into the reactor, a premixed gas mixture (2% CFC12 in argon, Alphagaz) was diluted with air and used, while a bubbler containing liquid CFC11 was used to feed CFC11 (b.p. 23.7°C) into the reactor by bubbling air or N_2 through it to vaporize CFC11 for its passage into the reactor.

The zeolite catalyst pellets were diluted with inert low surface area (0.15–0.35 m^2/g) alumina pellets (8–14 mesh size, obtained from Norton Co.) to form the catalyst bed for the deactivation studies. All the deactivation studies were carried out at a temperature of 300°C and a total gas flow rate of ~500 cc/min through the reactor. The amount of active zeolite catalyst was varied to achieve a range of space velocities (5000 to 30000 h^{-1}) through the reactor. The space velocities and the respective amounts of catalyst used for the deactivation studies are shown in Table 1. The approximate duration of most of the deactivation experiments was 7 h.

Analysis of the reactor inlet and effluent gas mixtures during the deactivation studies was performed using a Hewlett Packard 5890 GC with a Hewlett Packard 5970 MS. Calibration gas standards were also injected into the GC/MS to quantify the amounts of CFCs, CO_2, CCl_4, etc. in the reactor inlet and outlet streams as well. Details of the analytical techniques were discussed in an earlier work (4).

Various characterizations of the H–Y and the Cr–Y zeolite catalysts were performed after both 1 h and 7 h of deactivation. The zeolite catalyst pellets were diluted with inert alumina pellets to form the catalyst bed for the deactivation studies. Because it was cumbersome to separate them and obtain the pure deactivated catalyst for analysis at the end of the deactivation experiment, fresh catalyst pellets were subsequently charged to the reactor (without any inert diluent) and CFC/air mixture was passed through the reactor at the same concentration (1500–2000 ppm), temperature (300°C), and space velocity (5000 h^{-1}) in order to similarly deactivate them. Experiments were repeated twice with fresh catalyst to obtain 1 h and 7 h deactivated samples. After CFC/air mixture was passed for a specified duration (i.e., 1 h or 7 h), N_2 at 300°C was passed through the catalyst bed for a period of about 10–12 h to substantially desorb the adsorbed species from the catalyst surface. The deactivated catalyst pellets were stored in a desiccator for further characterization studies. Explanations for notations used

TABLE 1

Details of the Deactivation Experiments

Experiment #	Catalyst	Feed	Catalyst amount, vol in cm^3 (wt in g)	Space velocity, h^{-1}
1	H–Y	CFC11	6.0 (~3.0)	5000
2	H–Y	CFC12	6.0 (~3.0)	5000
3	Cr–Y	CFC11	6.0 (~3.0)	5000
4	Cr–Y	CFC12	6.0 (~3.0)	5000
5	H–Y	CFC11	1.0 (~0.5)	30000
6	Cr–Y	CFC12	2.9 (~1.4)	10500

TABLE 2

Notations for the Deactivated Zeolite Catalysts

Notation	Catalyst	Feed	Duration of deactivation, h	Catalyst amount, vol in cm^3 (wt in g)	Space velocity, h^{-1}
H–Y/CFC11/1 H	H–Y	CFC11	1	6.0 (~3.0)	5000
H–Y/CFC12/1 H	H–Y	CFC12	1	6.0 (~3.0)	5000
H–Y/CFC11/7 H	H–Y	CFC11	7	6.0 (~3.0)	5000
H–Y/CFC12/7 H	H–Y	CFC12	7	6.0 (~3.0)	5000
Cr–Y/CFC11/1 H	Cr–Y	CFC11	1	6.0 (~3.0)	5000
Cr–Y/CFC12/1 H	Cr–Y	CFC12	1	6.0 (~3.0)	5000
Cr–Y/CFC11/7 H	Cr–Y	CFC11	7	6.0 (~3.0)	5000
Cr–Y/CFC12/7 H	Cr–Y	CFC12	7	6.0 (~3.0)	5000

with the various deactivated samples (H–Y/CFC11/1 H, etc.) are shown in Table 2.

As briefly discussed below, the fresh and the deactivated zeolite catalysts were subjected to various characterizations (surface area, chromia content, acidity, IR, and XRD) to compare the changes in the properties as a function of deactivation time, type of feed, and catalyst.

The specific surface areas of the fresh and the deactivated catalysts were determined using a Quantachrome BET surface area analyzer. The Cr_2O_3 contents of the fresh and the deactivated Cr–Y catalysts were obtained using a Philips PV9550 X-ray fluorescence (XRF) spectrometer. The surface areas and the Cr_2O_3 contents of the various catalysts are tabulated in Table 3.

The acid strengths of the zeolite samples were determined by temperature programmed desorption (TPD) of NH_3. The TPD experiments were carried out in a DuPont model 2100 Thermal Analyst system with model 2950 Thermogravimetric Analyzer (TGA). The overall process involved degassing the sample at 500°C for 3 h in N_2, NH_3 adsorption at 100°C for 3 h, removal of physisorbed NH_3 by passing N_2 over the sample at 100°C for ~12 h, and finally, desorption of chemisorbed NH_3 from the sample by heating from 100°C to 550°C at a constant temperature ramp of 10°C/min.

IR spectra of the fresh and the deactivated samples were obtained using 9 mm diameter KBr diluted pellets. 20 mg of each sample were mixed with 2 g of KBr (1 : 100 dilution), and 29 mg of that mixture were used to prepare the pellets. Spectra were recorded with a Bio-rad FTS-7 FTIR spectrometer.

A Philips PW1710 X-ray diffractometer with Cu$k\alpha$ radiation was used to obtain the crystallinity of each sample.

RESULTS

The initial activity and selectivity, and also their changes with reaction time due to catalyst deactivation, for both the H–Y and the Cr–Y catalysts were discussed in our earlier publication (4). The primary focus of this study is on the changes in the properties of these two

TABLE 3

Properties of the Fresh and Deactivated H–Y and Cr–Y

Catalyst	Cr, as Cr_2O_3, wt% (σ = ±0.01 – 0.02)	Surface area, m^2/g (σ = ±4 – 7)	Acidity, NH_3 desorbed, mg/g of catalyst (σ = ±2 – 4)
Fresh H–Y		641	65
H–Y/CFC11/1 H		554	58
H–Y/CFC12/1 H		590	57
H–Y/CFC11/7 H		254	26
H–Y/CFC12/7 H		298	28
Fresh Cr–Y	2.15	467	39
Cr–Y/CFC11/1 H	2.10	462	45
Cr–Y/CFC12/1 H	2.08	469	46
Cr–Y/CFC11/7 H	1.84	422	50
Cr–Y/CFC12/7 H	1.76	430	48

zeolite catalysts as they deactivated during the oxidative destruction of CFCs. Potential relationships between these property changes and the observed changes in the catalytic activity and the product selectivity are also discussed briefly.

CFC11 Deactivation Results

Figures 1 and 2 show the changes in the catalytic activity and product selectivity for both H–Y and Cr–Y during the six deactivation experiments listed in Table 1. Experiments 1 and 3 compared the deactivation effect of CFC11 feed on the H–Y and Cr–Y catalysts at a temperature of 300°C and a space velocity of 5000 h^{-1}. From Fig. 1, it can be noticed that the initial conversion of CFC11 was 100% for both of the catalysts. However, after ~7 h, it was reduced to ~95% on the H–Y catalyst and to ~97% on the Cr–Y catalyst.

The experiment with CFC11 feed was repeated on the H–Y catalyst at a higher space velocity of 30000 h^{-1}, i.e., at a lower level of conversion (Experiment 5 of Table 1), to check whether any increase in activity, as observed in the case of CFC12 feed (discussed in the next section), was present initially. As shown in Fig. 1, no such trend was observed. An initial conversion of 92% was obtained at 30000 h^{-1} space velocity and the conversion continued to decrease with time, reaching ~22% after ~4.7 h.

Although the activity of the H–Y and the Cr–Y catalysts did not show much loss during the oxidative destruction of CFC11, reductions in the CO_2 selectivities were considerably more prominent (Fig. 2), falling from 100% to ~8% after ~7 h on the H–Y catalyst, and from 100% to ~65% on the Cr–Y catalyst. The other products detected with the reduction in CO_2 selectivity and their relative amounts were as follows: $CCl_4 > COCl_2 >$ traces of CFC12 on H–Y, and $COCl_2 > CCl_4 >$ CFC12 > traces of CFC13/CFC14[2] on Cr–Y.

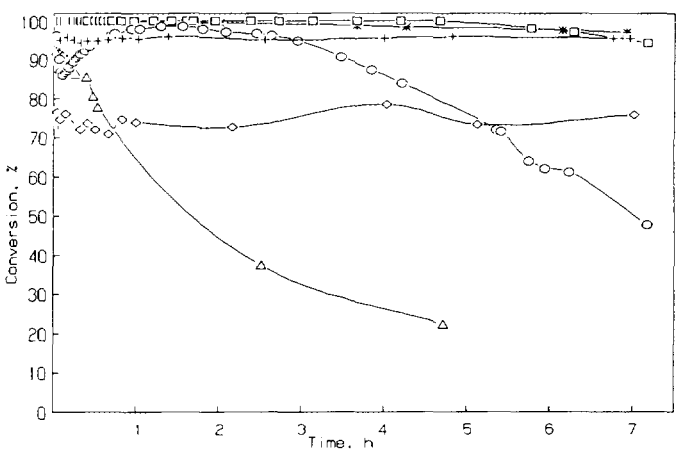

FIG. 1. Activity of H–Y and Cr–Y with time for CFC11 and CFC12 feeds at 300°C: [□] H–Y/CFC11(Expt. 1), [○] H–Y/CFC12(Expt. 2), [*]Cr–Y/CFC11(Expt. 3), [+] Cr–Y/CFC12(Expt. 4), sp vel = 5000 h^{-1}; [◇] Cr–Y/CFC12(Expt. 6), sp vel = 10500 h^{-1}; [△] H–Y/CFC11(Expt. 5), sp vel = 30000 h^{-1}.

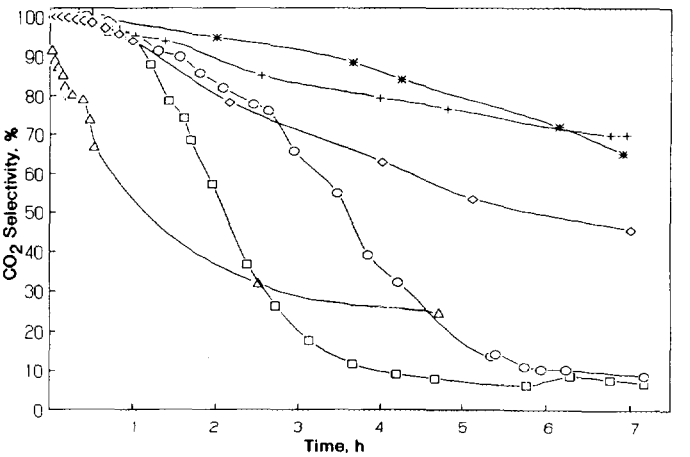

FIG. 2. CO_2 Selectivity for H–Y and Cr–Y with time for CFC11 and CFC12 feeds at 300°C: [□] H–Y/CFC11(Expt. 1), [○] H–Y/CFC12(Expt. 2), [*]Cr–Y/CFC11(Expt. 3), [+] Cr–Y/CFC12(Expt. 4), sp vel = 5000 h^{-1}; [◇] Cr–Y/CFC12(Expt. 6), sp vel = 10500 h^{-1}; [△] H–Y/CFC11(Expt. 5), sp vel = 30000 h^{-1}.

CFC12 Deactivation Results

Experiments 2 and 4 (Table 1) compare the deactivation effect of CFC12 feed on the H–Y and the Cr–Y catalysts again at 300°C and a space velocity of 5000 h^{-1}. The observed conversion of CFC12 with time on the H–Y zeolite catalyst showed drastically different behavior from that on Cr–Y, first increasing from an initial conversion of ~85% to ~98% after about an hour and slowly decreasing thereafter. Conversely, the Cr–Y catalyst showed a constant conversion of 95–96% for the CFC12 feed over the entire 7 h duration of the deactivation experiment.

Since the conversion of CFC12 on the Cr–Y catalyst was close to 100% at 5000 h^{-1} space velocity, the experiment was repeated at the same temperature of 300°C, but at a higher space velocity of 10500 h^{-1} (Experiment 6 in Table 1) to check whether any initial trend in the conversion of CFC12 (similar to that on the H–Y zeolite) could be noticed at a lower conversion level. It is obvious from Fig. 1 that no such trend exists even at a higher space velocity; a constant conversion of 72–78% was maintained during the 7 h period.

Conversely, deep oxidation selectivity (i.e., to CO_2) during CFC12 oxidation consistently dropped with time

[2] The general purpose fused silica capillary column (HP Ultra 1) used in the GC was incapable of separating CFC13 ($CClF_3$) and CFC14 (CF_4). Therefore, the small amounts of these gases produced during the deactivation studies could not be quantified separately and are referred to as CFC13/CFC14.

for both of these catalysts (Fig. 2). On the H–Y zeolite catalyst CO_2 selectivity fell steadily from 100% initially to ~10% after ~7 h, whereas on the Cr–Y zeolite catalyst, the reduction was less drastic (from 100% to ~70%). The other products detected with the fall in CO_2 selectivity, in decreasing order of magnitude, were CCl_4 > $COCl_2$ > CFC11 on H–Y, and CFC13/CFC14 > $COCl_2$ > CFC11 > CCl_4 on Cr–Y. During both CFC11 and CFC12 deactivation experiments only HCl was detected from the H–Y catalyst, while both HCl and Cl_2 were detected from the Cr–Y catalyst.

Properties of Deactivated Catalysts

To compare the properties of the deactivated catalysts with those of the fresh ones, deactivated catalyst samples were prepared by passing a CFC/air mixture (~2000 ppm CFC) over the respective catalysts at a temperature of 300°C and a space velocity of 5000 h^{-1} for 1 h and 7 h, respectively. In the following text, any catalyst properties "after 1 h" indicate properties of the 1-h deactivated catalyst samples and similarly properties "after 7 h" indicate those at the end of 7 h. Specific surface areas of both the fresh and deactivated H–Y and Cr–Y zeolites, along with chromia contents of the Cr–Y zeolites, are compared in Table 3.

Surface area. The original surface area of 641 m^2/g for the H–Y zeolite diminished to 554 m^2/g after 1 h of deactivation with the CFC11 feed and to 254 m^2/g after 7 of operation. Oxidative destruction of CFC12 feed on the H–Y zeolite caused the original surface area to decrease to 590 m^2/g after 1 h and to 298 m^2/g after 7 h of continuous operation.

The decline in surface area was much less in the case of Cr–Y zeolite. The original surface area of the Cr–Y zeolite was 467 m^2/g. After 1 h of CFC11 destruction, it was found to be 462 m^2/g and after 7 h, 422 m^2/g. For CFC12, the estimated surface areas of the Cr–Y zeolite were 469 and 430 m^2/g after 1 h and 7 h of destruction, respectively.

Chromia content. Chromia content of the Cr–Y zeolite also dropped with reaction time. As can be seen from Table 3, the original chromia content of the Cr–Y zeolite, which was 2.15%, diminished to 2.10% after 1 h of CFC11 destruction and to 1.84% after 7 h of CFC11 destruction. Similarly, CFC12 destruction on the Cr–Y catalyst caused the chromia content to fall to 2.08% after 1 h and to 1.76% after 7 h of operation.

Acidity. Acidities of the fresh and deactivated H–Y and Cr–Y catalysts are compared in Figs. 3a and 3b, respectively. The NH_3 TPD spectra consist of a distinct peak with a high temperature shoulder, and latter being less distinct in most of the spectra. Therefore, temperature shifts in the distinct peak have been correlated with increase or decrease in acidic strength of the zeolite catalysts. Figure 3a indicates that after 1 h of operation, the strength of the acidic sites, represented by the higher NH_3 desorption peak temperature, increased, particularly with the CFC12 feed (225°C as compared to 164°C for fresh H–Y). Conversely, the total acidity (the total amount of NH_3 desorbed being represented by the area under the curve) of the H–Y zeolite catalyst decreased continually with exposure to both CFC11 and CFC12 feeds (Fig. 3a and Table 3).

Comparison of Figs. 3a and 3b shows that the strength of the acidic sites for the fresh Cr–Y zeolite was higher than that for the fresh H–Y zeolite, with NH_3 desorption

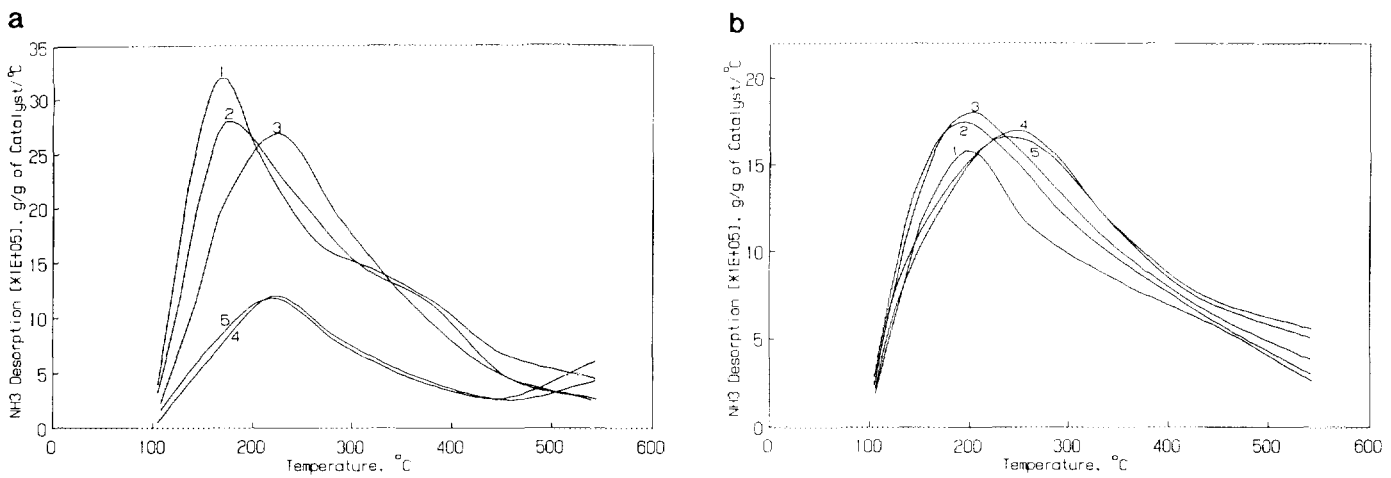

FIG. 3a. Acidity of fresh and deactivated H–Y determined by NH3 TPD: (1) H–Y, (2) H–Y/CFC11/1 H, (3) H–Y/CFC12/1 H, (4) H–Y/CFC11/7 H, and (5) H–Y/CFC12/7 H.

FIG. 3b. Acidity of fresh and deactivated Cr–Y determined by NH3 TPD: (1) Cr–Y, (2) Cr–Y/CFC11/1 H, (3) Cr–Y/CFC12/1 H, (4) Cr–Y/CFC11/7 H, and (5) Cr–Y/CFC12/7 H.

peak temperatures of 198 and 164°C, respectively. In contrast to the H–Y zeolite catalyst, the acidic strength of the Cr–Y did not increase after 1 h of deactivation with either CFC11 or CFC12, although it did undergo a modest increase in total acidity (Fig. 3b and Table 3). However, 7 h of CFC11/CFC12 destruction caused an appreciable increase in acidic strength of the Cr–Y zeolite (Fig. 3b) along with an increase in the total acidity (Fig. 3b and Table 3).

IR spectra. The structural IR spectra of the fresh and the deactivated H–Y and Cr–Y zeolite catalysts are illustrated in Figs. 4a and 4b, respectively. It is well known that in the IR spectra of zeolites in the wave number range of 300–1300 cm^{-1}, zeolite lattice vibrations can be observed, some of which are structure sensitive (26). Structural dealumination of zeolites causes these structure sensitive bands to shift to higher wave numbers. Peak broadening and reduction in intensity of these bands indicate framework disruption and a high concentration of defects.

It can be observed from Fig. 4a that after 1 h of oxidative destruction reaction on the H–Y zeolite, neither CFC11 nor CFC12 feed caused any appreciable structural dealumination as indicated by no shift in the band positions. However, after 7 h of deactivation, substantial dealumination and framework disruption were observed. The original bands at 1040, 895, and 580 cm^{-1} moved to 1080, 926, and 595 cm^{-1}, respectively. The band at 1150 cm^{-1} underwent a frequency shift and peak broadening as well. Also, the original bands at 737 and 507 cm^{-1} disappeared after 7 h of deactivation. Although no appreciable frequency shift was observed for the bands at 799 and 459 cm^{-1}, appreciable peak broadening could be detected.

As shown in Fig. 4b, the shift in the bands was much less in the case of Cr–Y catalyst. This indicates a lesser degree of dealumination, as the wave number has been reported to maintain a linear relationship with the number of lattice aluminum atoms in the case of Y zeolites (26). No dealumination of the Cr–Y catalyst was detected during 1 h of operation with both CFC11 and CFC12 feeds. However, after 7 h of operation, some slight dealumination and structure loss could be detected, as evidenced by the small shifts in the original bands at 1068 and 901 cm^{-1} and the broadening of the peaks at 822, 604, and 521 cm^{-1}.

XRD. Figures 5a and 5b represent the X-ray diffraction spectra of the fresh and deactivated H–Y and Cr–Y catalysts. During the first hour of CFC11 and CFC12 destruction, the H–Y catalyst experienced a loss of ~40% crystallinity (calculated based on the reduction in the peak height at $23.5° = 2\theta$) (Fig. 5a). However, after 7 h of operation, H–Y zeolite apparently lost all its crystallinity, as evidenced by the disappearance of all the characteristic peaks.

Conversely, no appreciable drop in the peak intensities (<5%) of the Cr–Y zeolite could be noticed during the first hour of CFC11 and CFC12 destruction, as indicated in Fig. 5b. However, after 7 h of CFC11 and CFC12 destruction, ~38% reduction in crystallinity was noticed.

DISCUSSION

From the activity and selectivity trends during the deactivation experiments and the property data of the fresh and deactivated catalysts, it can be concluded that Cr–Y is much more stable than H–Y during the oxidative destruction of CFC11 and CFC12 feeds.

The deactivation of the zeolite catalysts noticed during CFC oxidation was not merely the result of a direct reaction between the zeolite and the CFC reactant itself. Ear-

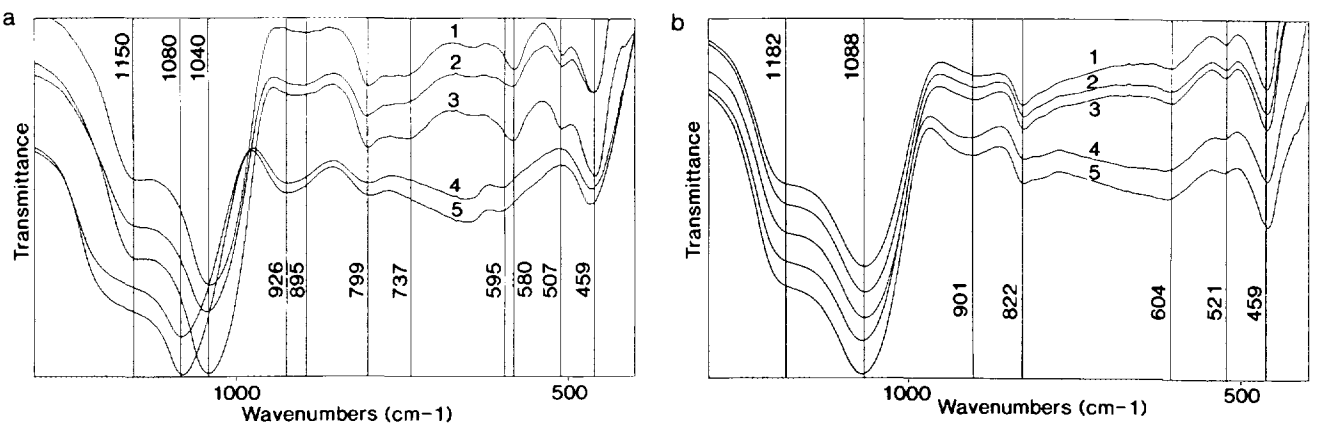

FIG. 4a. Framework IR spectra of fresh and deactivated H–Y: (1) H–Y, (2) H–Y/CFC11/1 H, (3) H–Y/CFC12/1 H, (4) H–Y/CFC11/7 H, and (5) H–Y/CFC12/7 H.

FIG. 4b. Framework IR spectra of fresh and deactivated Cr–Y: (1) Cr–Y, (2) Cr–Y/CFC11/1 H, (3) Cr–Y/CFC12/1 H, (4) Cr–Y/CFC11/7 H, and (5) Cr–Y/CFC12/7 H.

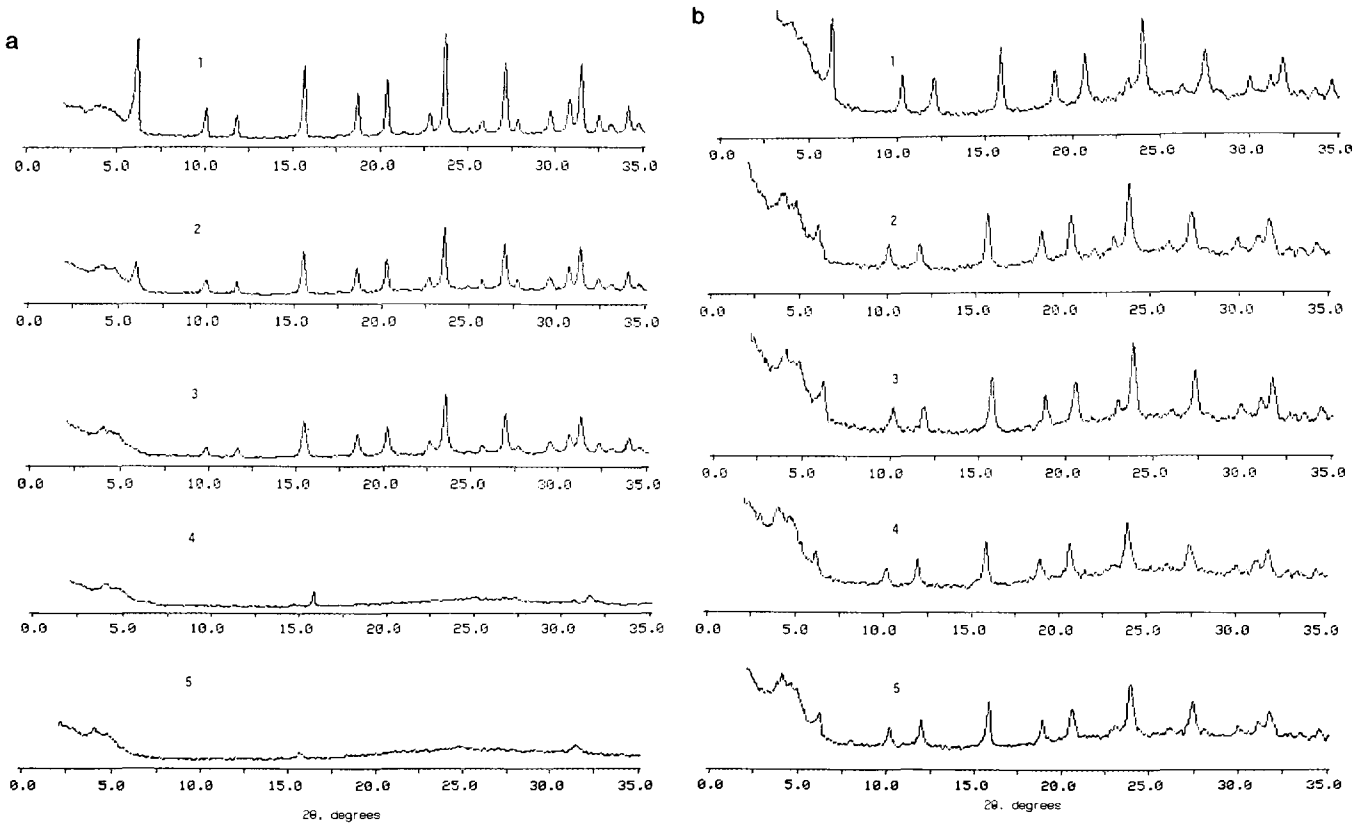

FIG. 5a. X-ray diffraction spectra of fresh and deactivated H–Y: (1) H–Y, (2) H–Y/CFC11/1 H, (3) H–Y/CFC12/1 H, (4) H–Y/CFC11/7 H, and (5) H–Y/CFC12/7 H.

FIG. 5b. X-ray diffraction spectra of fresh and deactivated Cr–Y: (1) Cr–Y, (2) Cr–Y/CFC11/1 H, (3) Cr–Y/CFC12/1 H, (4) Cr–Y/CFC11/7 H, and (5) Cr–Y/CFC12/7 H.

lier experiments carried out in our laboratory with and without air in the feed stream resulted in different initial CO_2 selectivities ($\geq$45% with air and <5% without air at 300°C), indicating oxygen from the air and not from the zeolite framework to be the primary oxidant. Therefore, deactivation was mostly due to influence of the corrosive reaction products formed during oxidation of CFCs. It should also be pointed out that there was no significant or visible coking, nor was deactivation reversible on heating the catalyst in air. The changes in the various properties of the two zeolites are discussed in the following section and are also compared with respect to changes in catalytic activity.

H–Y and Cr–Y Following First Hour of CFC11 and CFC12 Destruction

The most distinguishing feature observed was the increase in the acidic strength of the H–Y zeolite after the first hour of CFC12 destruction, as shown in Fig. 3a. This increase may have been responsible for the observed initial increase in CFC12 conversion on the H–Y catalyst (Fig. 1). The partial replacement of the zeolite oxygen and/or hydroxyls by more electronegative fluorine was the most probable reason for the increase in the acidic strength of the remaining hydroxyl sites. The absence of F_2 or HF in the reaction products and detection of fluorine in the catalyst after reaction[3] also suggested that fluorine was somehow trapped in the used catalyst. Other researchers have also reported (5–8, 10–24) increases in both Brønsted and Lewis acidity of zeolites and other metal oxide catalysts through incorporation of fluorine in them.

IR experiments carried out in our laboratory have shown that single carbon VOCs, such as CCl_4 and CH_2Cl_2, adsorb primarily on the Brønsted acid sites of zeolite Y (27, 28). IR experiments carried out during this study also confirmed adsorption of CFC12 on the

[3] The deactivated zeolite sample were leached with NaOH solution and leached solutions were later analyzed for the presence of fluoride ions using the ion selective electrode. Fluorine was detected (0.04–0.56 wt%) on all the deactivated catalysts listed in Table 2. The amount of fluorine in the catalyst increased with time, with the fluorine content of the feed (CFC12 > CFC11) and also with the type of catalyst (more on H–Y than on Cr–Y).

Brønsted acid sites of H–Y zeolite. The IR absorbance spectra of the zeolite hydroxyls are shown in Fig. 6 during CFC12 adsorption on H–Y zeolite at a temperature of 300°C. The dry and evacuated H–Y pellet was used as the reference for the spectra shown in Fig. 6. The negative hydroxyl peaks, particularly the negative peak at 3651 cm^{-1} (which corresponds to hydroxyls in the supercage), clearly indicated absorption of CFC12 on the acid sites. Following CFC12 adsorption on H–Y, vacuum was pulled for 1 h and the absence of change in the IR absorbance spectrum indicated that CFC12 was chemisorbed on the catalyst surface.

In his *in situ* IR study investigating the methylene chloride destruction mechanism, Chatterjee (27) proposed abstraction of zeolite hydroxyls leading to the formation of HCl. However, the hydroxyls were further replaced by the hydrogen present in the feed molecules or the water present in the reaction environment. Based on the IR and NMR results, Shepelev and Ione (29) also suggested a similar mechanism for the adsorption of methane on the zeolite acid sites during partial as well as complete oxidation of methane. Detection of HCl in the reactor effluent during dry CFC destruction also indicated participation of zeolite hydroxyls in the reaction. Therefore, it is possible that after CFC12 was adsorbed on the Brønsted acid site, it interacted with lattice, surface adsorbed, or gas phase oxygen, producing CO_2 and HCl. The fluorine, being strongly electronegative and very reactive, replaced the lattice oxygen and/or the hydroxyl and caused an increase in acidic strength.

The following simple mechanism is suggested for fluorination and subsequent acidity increase:

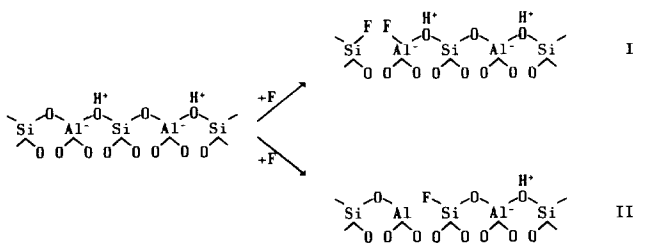

In reaction I, fluorine replaces the oxygen linked to aluminum and due to its strong electronegativity weakens the O–H bond, causing a higher proton mobility. In reaction II, fluorine replaces the hydroxyl group attached to aluminum (possibly changing it to a Lewis acid) and influences an adjacent Brønsted acid site. Becker and Kowalak (8) suggested that reaction I was primarily responsible for acidity increase of zeolite Y through fluorine modification. The overall process is perhaps more complex and not completely understood.

Unlike exposure of H–Y to CFC12 feed, exposure to CFC11 feed did not bring about any increase in activity of the H–Y zeolite at either space velocity (5000 and 30000

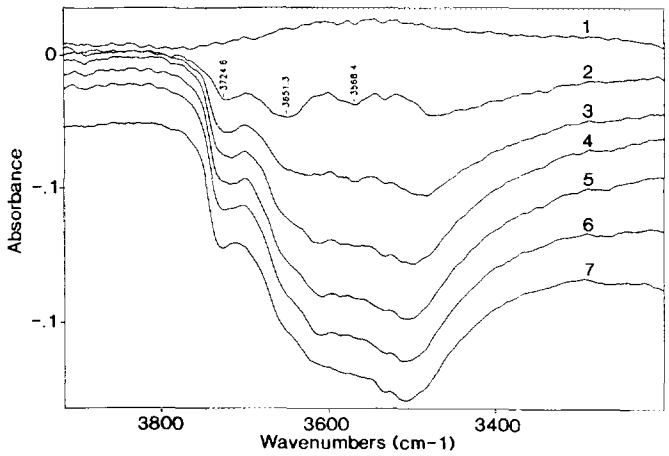

FIG. 6. IR spectra of H–Y with CFC12 adsorbing at 300°C. 1 = 0 min, 2 = 5 min, 3 = 10 min, ... 6 = 25 min of CFC12 adsorption, 7 = after 1 h of evacuation following 30 min of CFC12 adsorption.

h^{-1}) during the first hour of operation (Fig. 1). Since CFC11 has only one fluorine atom, compared to two in CFC12, at similar conversion levels (85–100%), the number of oxygen and/or hydroxyl groups replaced by fluorine would also be less in the case of CFC11 feed. That was perhaps the reason for the negligible increase in the acidic strength of the H–Y zeolite during the first hour of CFC11 destruction (Fig. 3a). Therefore, any enhancement in the activity of the catalyst was also not noticed as hypothesized with CFC12 feed.

The Cr–Y zeolite, on the other hand, did not show any increase in activity or acidic strength during the first hour of either CFC11 or CFC12 destruction, although an increase in the total acidity was evident from Fig. 3b and also from Table 3. As seen from Figs. 3a and 3b, the fresh Cr–Y zeolite had stronger acidic sites than the fresh H–Y zeolite (NH_3 desorption peak temperatures of 198 versus ~164°C respectively). This increase in acidic strength in the Cr–Y was due to framework dealumination during cation exchange in $Cr(NO_3)_3$ solution (pH = ~2.3). This is corroborated by XRF data (the Si/Al ratio of H–Y was 1.27 compared to 1.32 for Cr–Y) and IR results where comparison of Figs. 4a and 4b reveals a substantial shift in the structure sensitive IR bands after chromium exchange of H–Y.

However, partial replacement of lattice oxygen and/or hydroxyls by fluorine during the first hour of CFC12 destruction did not significantly change the acidic strength of the Cr–Y zeolite, but only the population of the sites (Figs. 3b and Table 3). Becker and Kowalak (8) had also reported that mild fluorination of Al–Y (a cation exchanged Y zeolite) did not generate stronger sites than those existing before fluorination, but only increased the population of the strong sites. Therefore, it is probable that the number of acidic sites does not play as important

a role in the destruction of CFC12 as does the strength of the acidic sites. This would be consistent with the fact that Cr–Y did not show any increase in activity during the first hour of CFC12 destruction.

H–Y and Cr–Y Following 7 h of CFC11 and CFC12 Destruction

During the 7 h of CFC11 and CFC12 destruction, significant drops in catalytic activity, deep oxidation selectivity, and physical properties were noticed, primarily in the case of H–Y zeolite.

Although the apparent reduction in CFC11 conversion over time was comparatively small (<10%) on both the H–Y and the Cr–Y catalysts, significant decrease in CFC12 conversion (~50%) was observed on the H–Y catalyst (Fig. 1). The reason was probably the higher reactivity of CFC11 feed as compared to CFC12, due to the presence of only one C–F bond (which is stronger than a C–Cl bond) compared to two in CFC12. Due to its higher reactivity, CFC11 could presumably remain at full conversion even though some catalyst deactivation had already occurred, as evidenced by the property changes.

Comparison of Figs. 1 and 2 shows that for both the catalysts and for both the feeds, the reduction in deep oxidation selectivity after 7 h was always significantly higher than the reduction in activity. Experiments carried out more recently in our laboratory with water in the feed stream showed substantial improvement in deep oxidation selectivity. For both H–Y and Cr–Y, it remained >90% even after 7 h of operation. It is possible that water inhibited the formation of other intermediates or by-products, such as $COCl_2$, CCl_4, CFC13/14, etc., and since in this study no water was present in the feed stream, participation and continuous consumption of zeolitic water, as mentioned earlier, eventually caused the fall in CO_2 selectivity.

Stability of the Cr–Y catalyst was much higher than that of the H–Y catalyst, as evidenced by the lesser drop in activity (Fig. 1), deep oxidation selectivity (Fig. 2), and the various properties (Figs. 3a–5b). The presence of Cr^{3+}, a polyvalent cation, apparently imparted greater structural stability to Cr–Y, as three alumina tetrahedra are bonded to one chromium cation. Improved stability of polyvalent cation exchanged zeolites was also observed by Kowalak *et al.* (5–8). The Deacon reaction, characteristic of Cr^{3+} ions present in Cr–Y, also probably conferred improved stability on the Cr–Y zeolite. Since no water was added in the reactant stream, the expected reaction products were CO_2, Cl_2, and F_2. However, only HCl was detected in the product stream of H–Y zeolite indicating reaction between Cl_2 and zeolite hydroxyls. Conversely, Cr–Y produced a substantial amount of Cl_2 along with some HCl (4). Therefore, the HCl produced on Cr–Y (a good Deacon catalyst) was further converted to Cl_2, restoring the zeolite hydroxyls and thereby conferring better stability on the Cr–Y zeolite.

Any F_2 and HF formed were mostly trapped in the catalysts and were not detected in the effluent stream. Although no fluorine-containing products were detected from the H–Y catalyst, 0–300 ppm CFC13/14 was detected from the Cr–Y catalyst, indicating lesser retention of fluorine by the Cr–Y catalyst. Analysis of the 7-h deactivated catalysts for fluorine content also showed slightly higher fluorine retention on the H–Y (0.36–0.56 wt%) than on the Cr–Y (0.31–0.52 wt%). The lesser retention of fluorine on Cr–Y probably caused lesser dealumination and hence provided better stability to this catalyst.

Figure 3b shows an increase in the acidic strength and in the total acidity of the Cr–Y zeolite after 7 h of CFC11 and CFC12 destruction. These increases did not increase activity, probably due to the combined effects of loss in chromia content and surface area (Table 3).

XRF analysis of the deactivated zeolite catalysts as compared to the fresh zeolite samples did not show measurable change in the Si/Al ratios. Since silicon halides are more volatile as compared to aluminum, no change in the Si/Al ratios indicated negligible loss of silica from the catalyst as volatile halides. Detection of a very small quantity of SiF_4 in the GC/MS (probably ≤10 ppm, although the GC/MS was not calibrated to quantify) also supported the consistency of the Si/Al ratios. Therefore, based on all these observations, it is suggested that structure collapse and subsequent loss in crystallinity and surface area of the zeolite catalysts took place primarily through dealumination. The process of dealumination is probably complicated; however, a simple mechanism suggested by Kowalak *et al.* (8) is shown below:

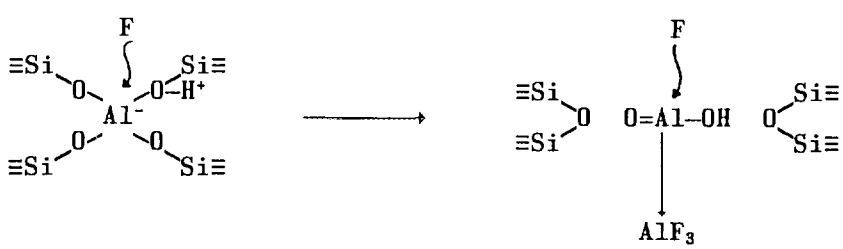

The structural collapse of zeolite catalysts with successive loss in surface area and active reaction sites resulted in catalyst deactivation, as evidenced by reduction in activity and deep oxidation selectivity. Since dealumination and hence structural collapse were much less severe in the case of Cr–Y zeolite, the corresponding catalyst deactivation was also less significant as campared to that for the H–Y zeolite.

ACKNOWLEDGEMENTS

Partial funding for this research was obtained from the U.S. Environmental Protection Agency and the U.S. Air Force and is acknowledged with appreciation. Zeolite samples were supplied by UOP.

REFERENCES

1. Chatterjee, S., and Greene, H. L., *J. Catal.* **130,** 76 (1991).
2. Chatterjee, S., Greene, H. L., and Park, Y. J., *J. Catal.* **138,** 179 (1992).
3. Chatterjee, S., and Greene, H. L., *Appl. Catal.* **98,** 139 (1993).
4. Karmakar, S., and Greene, H. L., *J. Catal.* **138,** 364 (1992).
5. Kowalak, S., *J. Chem. Soc. Faraday Trans. 1* **84**(6), 2035 (1988).
6. Fiedorow, R., Kowalak, S., and Kozlowski, M., *React. Kinet. Catal. Lett.* **34**(1), 81 (1987).
7. Becker, K. A., and Kowalak, S., *J. Chem. Soc. Faraday Trans. 1* **83,** 535 (1987).
8. Becker, K. A., and Kowalak, S., "Recent Advances in Zeolite Science," p. 123. Elsevier, Amsterdam/New York, 1989.
9. Fevrier, D., Mignon, P., and Vernet, J. L., *J. Catal.* **50,** 390 (1977).
10. Kowalak, S., and Ziolek, M., *Zeolites* **7,** 535 (1987).
11. Kowalak, S., *Chem. Stosow.* **34** (1–2), 93 (1990).
12. Balkus, K. J., Jr., Nowinska, K., and Kowalak, S., *Catal. Lett.* **9,** 145 (1991).
13. Becker, K. A., and Kowalak, S., *Acta Chim. Hung.* **125**(6), 869 (1988).
14. Kowalak, S., and Moffat, J. B., *Appl. Catal.* **36.** 139 (1988).
15. Becker, K. A., and Kowalak, S., *J. Chem. Soc. Faraday Trans. 1* **82,** 2151 (1986).
16. Becker, K. A., and Kowalak, S., *J. Chem. Soc. Faraday Trans. 1* **81,** 1161 (1985).
17. Becker, K. A., Fabianska, K., and Kowalak, S., *in* "Meterogeneous Catalysis: Proceedings of the Sixth International Symposium," Part 2, p. 187 (1987).
18. Ghosh, A. K., and Kydd, R. A., *J. Catal.* **103,** 399 (1987).
19. Ghosh, A. K., and Kydd, R. A., *Catal. Rev. Sci. Eng.* **27** (4), 539 (1985).
20. Lok, B. M., Gortsema, F. P., Messina, C. A., Rastelli, H., and Izod, T. P. J., "Intrazeolite Chemistry," ACS Symposium Series 218, p. 41. Washington, D.C., 1983.
21. Lok, B. M., and Izod, T. P. J. *Zeolites* **2,** 66 (1982).
22. Kurosaki A., and Okazaki, S., *Bull. Chem. Soc. Jpn.* **63,** 2363 (1990).
23. Kurosaki, A., and Okazaki, S., *Chem. Lett.*, 589 (1991).
24. Kodama, H., and Okazaki, S., *J. Catal.* **132,** 512 (1991).
25. "Ion Exchange and Metal-Loading Procedure," Linde Molecular Sieves Catalyst Bulletin, 1988.
26. Flanigen, E. M., "Zeolite Chemistry and Catalysis," Chap-2. ACS Monograph No. 171, Amer. Chem. Soc., Washington, DC, 1976.
27. Chatterjee, S. Doctoral Dissertation, Univ. of Akron, 1993.
28. Ramachandran, B. Master's Thesis, Univ. of Akron, 1993.
29. Shepelev, S. S., and Ione, K. G., *J. Catal.* **117,** 362 (1989).